

Magnetic hysteresis of blocked ferrihydrite nanoparticles

Cite as: AIP Advances **11**, 015329 (2021); <https://doi.org/10.1063/9.0000111>

Submitted: 15 October 2020 • Accepted: 10 December 2020 • Published Online: 11 January 2021

 S. V. Komogortsev, D. A. Balaev, A. A. Krasikov, et al.



View Online



Export Citation



CrossMark

ARTICLES YOU MAY BE INTERESTED IN

[Influence of magnetic nanoparticles on cells of Ehrlich ascites carcinoma](#)

AIP Advances **11**, 015019 (2021); <https://doi.org/10.1063/9.0000165>

[Crystalline structure and magnetic properties of pyrite FeS₂](#)

AIP Advances **11**, 015131 (2021); <https://doi.org/10.1063/9.0000110>

[Structural and magnetic properties of iodide-mediated chemically synthesized L1₂ FePt₃ nanoparticles](#)

AIP Advances **11**, 015312 (2021); <https://doi.org/10.1063/9.0000102>

Call For Papers!

AIP Advances

SPECIAL TOPIC: Advances in
Low Dimensional and 2D Materials

Magnetic hysteresis of blocked ferrihydrite nanoparticles

Cite as: AIP Advances 11, 015329 (2021); doi: 10.1063/9.0000111
Presented: 2 November 2020 • Submitted: 15 October 2020 •
Accepted: 10 December 2020 • Published Online: 11 January 2021



View Online



Export Citation



CrossMark

S. V. Komogortsev,^{1,a)}  D. A. Balaev,¹ A. A. Krasikov,¹ S. V. Stolyar,² R. N. Yaroslavtsev,² V. P. Ladygina,² and R. S. Iskhakov¹

AFFILIATIONS

¹Kirensky Institute of Physics, Russian Academy of Sciences, Siberian Branch, Krasnoyarsk 660036, Russia

²Krasnoyarsk Science Center, Russian Academy of Sciences, Siberian Branch, Krasnoyarsk 660036, Russia

Note: This paper was presented at the 65th Annual Conference on Magnetism and Magnetic Materials.

a) Author to whom correspondence should be addressed: komogor@iph.krasn.ru

ABSTRACT

Using minor hysteresis loops in the Stoner–Wohlfarth model allows describing the experimental behavior of the coercive force of minor hysteresis loops in ferrihydrite nanoparticles with a change in the field amplitude. The description allows estimating the parameters of the distribution of the magnetic anisotropy field in nanoparticles. The best agreement of the anisotropy fields estimated by different approaches is achieved for the assumption of uniaxial anisotropy in ferrihydrite nanoparticles.

© 2021 Author(s). All article content, except where otherwise noted, is licensed under a Creative Commons Attribution (CC BY) license (<http://creativecommons.org/licenses/by/4.0/>). <https://doi.org/10.1063/9.0000111>

I. INTRODUCTION

Ferrihydrite nanoparticles are characterized by negative exchange interactions and extremely high fields of reaching the major hysteresis loop, up to 10^5 kOe. The physics of hysteresis in these particles is not fully understood. Various ideas, such as spin glass shell effects^{1,2} and quantum tunneling^{3,4} are discussed. The experiment indicates an uncompensated magnetic moment $\langle\mu\rangle$ in a ferrihydrite nanoparticle. The $\langle\mu\rangle$ value was well studied by characterizing the magnetization curves for nanoparticles in the superparamagnetic state⁵ using equations containing Langevin functions. Magnetic studies according to the ZFC-FC protocol make it possible to estimate the blocking temperature for a certain measurement time, typical for the chosen measurement tool.^{6–8} Combined with the particle size, this allows one to estimate the effective magnetic anisotropy constant.^{7,9} For the nanoparticles in the deeply blocked state (at temperatures much lower than the blocking temperature) which are characterized by the magnetic moment and magnetic anisotropy constant, one can expect the behavior to be consistent with the Stoner–Wohlfarth model.^{10,11} The measurement of minor hysteresis loops in ferrihydrite nanoparticles is a tool for studying the potential relief which controls their reversible and irreversible magnetic behavior.

In this work, we use the Stoner–Wohlfarth model and idea concerning the anisotropy field distribution to describe the dependence of coercive force in minor hysteresis loop on the amplitude of the applied field for ferrihydrite nanoparticles.

II. EXPERIMENT

Three samples of ferrihydrite nanoparticles, namely, biogenic ferrihydrite (BFh), synthetic ferrihydrite (SFh) and synthetic ferrihydrite doped with cobalt (SFh-Co), were used, their preparation, characterization and experimental studies having been carried out by the authors earlier.¹²

The technique for preparing BFh nanoparticles formed during the vital activity of bacteria was described in detail in Refs. 13–15. The investigated BFh sample was annealed at a temperature of 150°C for 24 h.⁸ Synthetic ferrihydrites (SFh and SFh-Co) were prepared using the technique described in Refs. 12 and 16. The analysis of Mössbauer spectra allowed concluding that the studied samples were ferrihydrite ones without any foreign iron-containing phases.^{7,17} The magnetic measurements were performed using a vibrating sample magnetometer (VSM).¹⁸ The investigated powder sample was fixed in a measuring capsule using paraffin (the data obtained were corrected to the paraffin diamagnetic signal).

The cooling of the nanoparticles from the superparamagnetic state in the magnetic field was shown to lead to a significant bias of the loop, but the cooling in the zero field allowed one to obtain almost symmetric hysteresis loops.^{1,8} In this work, we studied a series of minor loops at $T = 4.2$ K starting from a completely demagnetized state achieved by cooling from the superparamagnetic state in the zero field. Starting from this point the series of minor loops were measured using a gradual increase in the applied field amplitude H_{\max} .

For the numerical calculation of the minor hysteresis loops within the Stoner–Wohlfarth model the software package the Object Oriented Micro Magnetic Framework (OOMMF) was used.¹⁹

III. RESULTS AND DISCUSSION

The magnetization behavior at low amplitude of the applied field (changing from $H_{\max} = 0$ according to the scenario $H_{\max} \rightarrow -H_{\max} \rightarrow H_{\max}$), demonstrates a linear reversible response (see the inset in Fig. 1). With the increasing H_{\max} , it becomes slightly nonlinear, and then, starting from a certain field, H_{\max}^* reveals hysteresis. Starting from this field H_{\max}^* , with a further increase in H_{\max} , the hysteresis increases, first rather quickly, then more and more slowly, which implies the approach to the major magnetic hysteresis loop (Fig. 1).

Qualitatively, this behavior agrees with the behavior of magnetic particles in the Stoner–Wohlfarth model.²⁰ In this model, the value of H_c is determined by the magnetic anisotropy field of a single particle H_a . The anisotropy field also determines the field of “opening” of the minor loop and the characteristic field of the transition to the major loop (see Fig. 2). This is used in the experiment to estimate the anisotropy field from H_c , the loop “opening” field and the major loop closing field.²¹ The difference in the shape of the experimental and model loops (see the insets in Fig. 2) may be associated with the presence of antiferromagnetic, spin-glass, and residual superparamagnetic responses in the nanoparticles, as well as

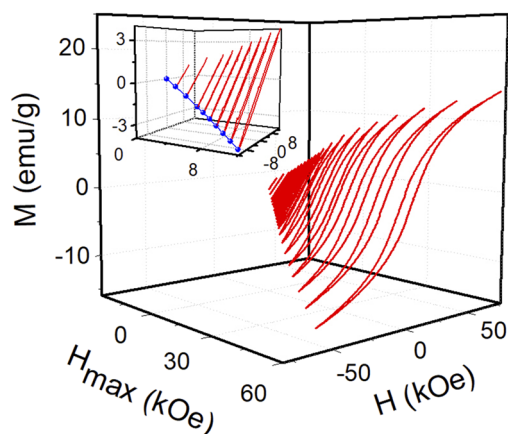


FIG. 1. The minor loops of synthetic ferrihydrite (SFh) exhibit the behavior typical of all the three samples (the series of loops for SFh-Co and BFh are given in [supplementary material 1](#)). The inset shows the region of low fields, where the transition from the reversible to irreversible behavior occurs.

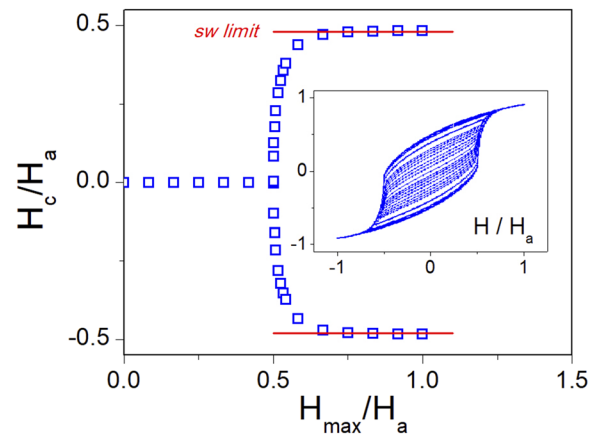


FIG. 2. The numerical behavior of the minor loop coercivity vs the applied field H_{\max} amplitude in the Stoner–Wohlfarth model. The case of randomly oriented particles with uniaxial magnetic anisotropy ($K > 0$). The insets show the calculated series of the minor loops used for plotting H_c vs H_{\max} .

with the distribution of the particle parameters. However, the qualitative similarity of the magnetic hysteresis behavior in the experiment and the model allows one to use this model to describe the dependence of the coercive force on the amplitude of the field H_{\max} in the minor loop.

A primary comparison of the model (Fig. 2) and experimental dependences of H_c on H_{\max} shows their significant difference. In the model, the field of “opening” of the minor loop H_{\max}^* and the characteristic field of the transition to the major loop are of the same order of magnitude (Fig. 2 shows only the case of uniaxial magnetic anisotropy ($K > 0$), the data on the cubic anisotropy case are given in [supplementary material 2](#)). In the experiment one can estimate the field H_{\max}^* at the level of 3–8 kOe, while the major loop is not reached even at 75–90 kOe.

The transition from opening the loop to reaching the major loop regime occurs very abruptly (Fig. 2) in comparison with the experimental behavior (Fig. 3). Such a slow mode of reaching the major loop in the experiment can be associated with the inhomogeneity of the anisotropy fields in the ensemble of nanoparticles. The coercive force is not a strictly additive characteristic, but averaging can be used in this case, assuming the hysteresis loops of the particles to be summed.²² We describe the elementary process of opening the loop using the Heaviside step function $S(x)$:

$$h_c(h_{\max}, H^*, H_c^{\text{inf}}) = H_c^{\text{inf}} \cdot S(h_{\max} - H^*). \quad (1)$$

Two ways are possible to estimate the distribution of the field H^* (which is related to the anisotropy field as $H_a^* = \beta \cdot H^*$). The first is the fitting of the experimental data using the integral function:

$$H_c(h_{\max}) = \frac{\int h_c(h_{\max}, H^*, H_c^{\text{inf}}) \cdot f(H^*) dH^*}{\int f(H^*) dH^*}, \quad (2)$$

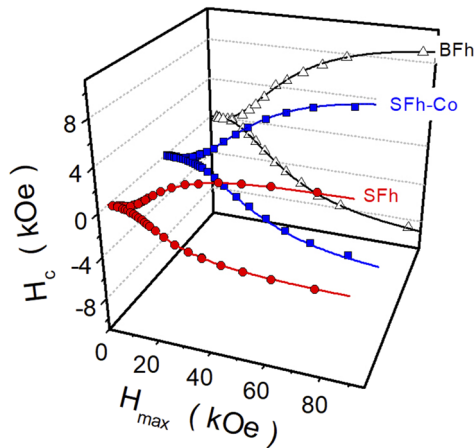


FIG. 3. The experimental coercivity vs the applied field amplitude in the minor loop (symbols) for various ferrihydrite nanoparticles and the fitting by Eq. (2) (lines).

where $f(H^*)$ is the distribution function of H^* . Figure 3 shows that Eq. (2) fits the data well for all the three samples of the nanoparticles. The lognormal distribution $f(H^*)$ was used in Eq. (2).

Similarly to the Stoner–Wohlfarth model, it is assumed that H^* and H_c^{inf} are correlated $H^* = \alpha H_c^{inf}$, where α is the constant for all the elementary processes of opening the minor loop.

The second way makes it possible to directly estimate the distribution function H^* . Since the derivative of $S(x)$ is a delta function, the distribution of the statistical weights of the H^* parameter can be estimated as:

$$f'(H^*) = \frac{1}{H_{max}} \cdot \frac{dH_c}{dH_{max}}. \tag{3}$$

The result of using Eq. (3) is shown by symbols in Fig. 4. The obtained H^* distribution is in good agreement both with the

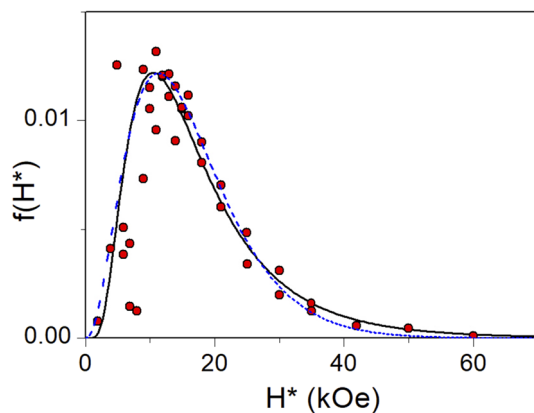


FIG. 4. The distribution of H^* obtained using the differentiation of the experimental dependence, Fig. 3 (symbols) is in good agreement with the lognormal function used in the best fit of the data by Eq. (2) (solid line) and with the gamma distribution (dashed line). The example of chemical ferrihydrite is used.

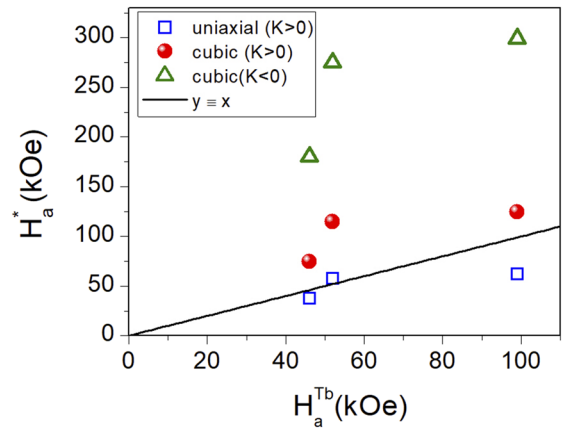


FIG. 5. The comparison of the anisotropy field H_a^* estimated as $H_a^* = \beta \cdot H^*$ (squares are to denote β for uniaxial anisotropy ($K > 0$), circles - cubic ($K > 0$), triangles - cubic ($K < 0$)) with the anisotropy field H_a^{Tb} estimated from the blocking temperature. The straight line corresponds to the equality of two values.

lognormal function used in Eq. (2) (with the distribution parameters corresponding to the best fit), and with the gamma distribution, which was discussed earlier as the most characteristic one for the anisotropy constant distribution for ferrihydrite nanoparticles.²³ The parameters of the lognormal distribution $f(H^*)$ corresponding to the best fit of the data by Eq. (2) for the ferrihydrite nanoparticles of three different types are the following: for BFh the average $H^* = 23$ kOe, the distribution width $\sigma = 0.65$; for SFh $H^* = 15$ kOe, the distribution width $\sigma = 0.6$ and for SFh-Co $H^* = 25$ kOe, the distribution width $\sigma = 0.6$.

The magnetic anisotropy field of the particle can be estimated as $H_a^* = \beta \cdot H^*$ using H^* for the best fitting by Eq. (2). The value of β in the Stoner–Wohlfarth model is different for the cases of uniaxial, cubic positive and negative anisotropy (see supplementary material 2); therefore, for each sample in Fig. 5, we have 3 different estimates (for different types of anisotropy). In Fig. 5, this value is compared with the anisotropy field determined from T_b and $\langle \mu_p \rangle$ (Table I) as: $H_a^{Tb} = 50 \cdot k_B \cdot T_b / \langle \mu_p \rangle$.

Fig. 5 shows that the estimate H_a^* from the Stoner–Wohlfarth model with uniaxial anisotropy is closer to the equality line. This result is consistent with the following observation. If we take the experimental values H^* without processing using Eq. (2) (H^* as the field H_{max} where magnetic hysteresis first appears) and H_c^{inf} estimated by extrapolation to infinite fields (see, for example,

TABLE I. The parameters of the studied nanoparticles determined in the Refs. 5, 7, and 8.

Sample	Particle size (nm)	$\langle T_b \rangle$ (K)	$\langle \mu_p \rangle (\mu_B)$
SFh	2.5	12	173
SFh-Co	3.5	9	145
BFh	4.5 ÷ 5	40	301

Refs. 1 and 8) we have $H_c^{inf}/H^* \approx 1$, which is close to the prediction of the Stoner–Wohlfarth model for uniaxial magnetic anisotropy ($H_c^{inf}/H^* \approx 0.96$).

IV. CONCLUSION

New findings resulting from the study of the minor hysteresis loops of ferrihydrite nanoparticles are reported. For the particles with the zero exchange bias, starting from the state with the zero average magnetic moment, a series of the minor loops were measured with a progressively increasing magnitude of the maximum field from 0.1 to 70 kOe. Biogenic, chemically synthesized and chemically synthesized Co-doped ferrihydrite nanoparticles were studied. At low field amplitude, a reversible magnetic response is observed. With increasing the field amplitude, the minor loops become open and then, they approach the major loop. Since this resembles the behavior of single-domain particles in the Stoner–Wohlfarth model, we tested this model to describe the dependence of the coercive force of the minor loop versus the field amplitude. Such a description is successful when the dispersion of the anisotropy field is taken into account. We also compared the anisotropy field obtained from this description with the estimate from the value of the blocking temperature. This makes it possible to evaluate the applicability framework of the Stoner–Wohlfarth model for the magnetic hysteresis description in ferrihydrite nanoparticles.

SUPPLEMENTARY MATERIAL

In the [supplementary material](#), the hysteresis loops are given, measured for all tested samples ([supplementary material 1](#)). The calculated minor and major hysteresis loops within the Stoner–Wohlfarth model, as well as the analysis of the main fields characterizing the reversible and irreversible behavior of the hysteresis loops are presented in [supplementary material 2](#).

ACKNOWLEDGMENTS

The magnetic measurements were partially carried out on the equipment of the Krasnoyarsk Regional Center for Collective Use, Krasnoyarsk Science Center, Siberian Branch, Russian Academy of Sciences. This study was supported by the Council of the President of the Russian Federation for State Support of Young Scientists and Leading Scientific Schools (project no. MK-1263.2020.3).

DATA AVAILABILITY

The data that support the findings of this study are available from the corresponding author upon reasonable request and available within the article and its [supplementary material](#).

REFERENCES

- N. J. O. Silva, V. S. Amaral, A. Urtizberea, R. Bustamante, A. Millán, F. Palacio, E. Kampert, U. Zeitler, S. de Brion, Ö. Iglesias, and A. Labarta, *Phys. Rev. B* **84**, 104427 (2011).
- H. Mamiya, I. Nakatani, and T. Furubayashi, *Phys. Rev. Lett.* **88**, 067202 (2002).
- F. Luis, E. del Barco, J. M. Hernández, E. Remiro, J. Bartolomé, and J. Tejada, *Phys. Rev. B* **59**, 11837 (1999).
- J. Tejada, X. X. Zhang, E. del Barco, J. M. Hernández, and E. M. Chudnovsky, *Phys. Rev. Lett.* **79**, 1754 (1997).
- D. A. Balaev, A. A. Krasikov, A. A. Dubrovskii, S. V. Semenov, O. A. Bayukov, S. V. Stolyar, R. S. Iskhakov, V. P. Ladygina, and L. A. Ishchenko, *J. Exp. Theor. Phys.* **119**, 479 (2014).
- D. A. Balaev, A. A. Krasikov, A. A. Dubrovskii, O. A. Bayukov, S. V. Stolyar, R. S. Iskhakov, V. P. Ladygina, and R. N. Yaroslavtsev, *Tech. Phys. Lett.* **41**, 705 (2015).
- D. A. Balaev, A. A. Krasikov, A. A. Dubrovskii, S. I. Popkov, S. V. Stolyar, O. A. Bayukov, R. S. Iskhakov, V. P. Ladygina, and R. N. Yaroslavtsev, *J. Magn. Magn. Mater.* **410**, 171 (2016).
- D. A. Balaev, A. A. Krasikov, A. A. Dubrovskii, S. I. Popkov, S. V. Stolyar, R. S. Iskhakov, V. P. Ladygina, and R. N. Yaroslavtsev, *J. Appl. Phys.* **120**, 183903 (2016).
- Y. V. Knyazev, D. A. Balaev, S. V. Stolyar, O. A. Bayukov, R. N. Yaroslavtsev, V. P. Ladygina, D. A. Velikanov, and R. S. Iskhakov, *J. Alloys Compd.* **851**, 156753 (2021).
- S. V. Komogortsev, T. N. Patrusheva, D. A. Balaev, E. A. Denisova, and I. V. Ponomarenko, *Tech. Phys. Lett.* **35**, 882 (2009).
- I. S. Poperechny, Y. L. Raikher, and V. I. Stepanov, *Phys. B Condens. Matter* **435**, 58 (2014).
- S. V. Stolyar, D. A. Balaev, V. P. Ladygina, A. A. Dubrovskii, A. A. Krasikov, S. I. Popkov, O. A. Bayukov, Y. V. Knyazev, R. N. Yaroslavtsev, M. N. Volochaev, R. S. Iskhakov, K. G. Dobretsov, E. V. Morozov, O. V. Falaleev, E. V. Inzhevatin, O. A. Kolenchukova, and I. A. Chizhova, *J. Supercond. Nov. Magn.* **31**, 2297 (2018).
- S. V. Stolyar, O. A. Bayukov, Y. L. Gurevich, V. P. Ladygina, R. S. Iskhakov, and P. P. Pustoshilov, *Inorg. Mater.* **43**, 638 (2007).
- Y. L. Raikher, V. I. Stepanov, S. V. Stolyar, V. P. Ladygina, D. A. Balaev, L. A. Ishchenko, and M. Balasoiu, *Phys. Solid State* **52**, 298 (2010).
- D. A. Balaev, A. A. Dubrovskii, A. A. Krasikov, S. V. Stolyar, R. S. Iskhakov, V. P. Ladygina, and E. D. Khilazheva, *JETP Lett.* **98**, 139 (2013).
- F. M. Michel, L. Ehm, S. M. Antao, P. L. Lee, P. J. Chupas, G. Liu, D. R. Strongin, M. A. A. Schoonen, B. L. Phillips, and J. B. Parise, *Science* **316**, 1726 (2007).
- S. V. Stolyar, R. N. Yaroslavtsev, R. S. Iskhakov, O. A. Bayukov, D. A. Balaev, A. A. Dubrovskii, A. A. Krasikov, V. P. Ladygina, A. M. Vorotynov, and M. N. Volochaev, *Phys. Solid State* **59**, 555 (2017).
- A. D. Balaev, Y. B. Boyarshinov, M. M. Karpenko, and B. P. Khrustalev, *Prib. Tekh. Eksp.* **3**, 167 (1985).
- M. J. Donahue and D. G. Porter, *OOMMF User's Guide*, Version 1.0, Gaithersburg, MD, 1999.
- E. C. Stoner and E. P. Wohlfarth, *Philos. Trans. Roy. Soc. A* **240**, 559 (1948).
- A. Harres, M. Mikhov, V. Skumryev, A. M. H. de Andrade, J. E. Schmidt, and J. Geshev, *J. Magn. Magn. Mater.* **402**, 76 (2016).
- S. V. Komogortsev, R. S. Iskhakov, A. D. Balaev, A. V. Okotrub, A. G. Kudashov, N. A. Momot, and S. I. Smirnov, *Phys. Solid State* **51**, 2286 (2009).
- N. J. O. Silva, V. S. Amaral, L. D. Carlos, B. Rodríguez-González, L. M. Liz-Marzán, T. S. Berquó, S. K. Banerjee, V. de Zea Bermudez, A. Millán, and F. Palacio, *Phys. Rev. B* **77**, 134426 (2008).